Spin-polarized Andreev molecules and anomalous nonlocal Josephson effects in altermagnetic junctions

Sayan Mondal and Jorge Cayao*

Department of Physics and Astronomy, Uppsala University, Box 516, S-751 20 Uppsala, Sweden

(Received 16 March 2026; accepted 23 July 2026; published 24 August 2026)

Altermagnetism has emerged as a promising ingredient for realizing nontrivial Josephson phases but so far explored in single Josephson junctions. In this work, we consider the coherent coupling of two Josephson junctions with spin-singlet s-wave superconductivity and demonstrate that d-wave altermagnetism gives rise to spin-polarized Andreev molecules due to the hybridization of Andreev bound states of each junction when the coupling is weak. Interestingly, these spin-polarized Andreev molecules induce anomalous nonlocal Josephson effect, where the current flow across one Josephson junction due to phase changes across the other junction develops $0-\pi$ and ϕ_0 transitions originating from altermagnetism. Furthermore, the nonlocal Josephson current carried by spin-polarized Andreev molecules exhibits nonreciprocal critical currents, enabling a nonlocal Josephson diode effect whose polarity is tunable by the altermagnetic strength and right phase. Our findings put forward altermagnetism as a promising arena for designing nonlocal spin Josephson phenomena.

DOI: 10.1103/l42w-8qrz

I. INTRODUCTION

The advent of altermagnetism has provided an unexplored front in the search for nontrivial superconducting phenomena that are promising for quantum applications [1,2]. This is because altermagnets (AMs) possess anisotropic spin-polarized Fermi surfaces and zero net magnetization [3–14], originated from a collinear-compensated magnetic ordering in real space that preserves inversion symmetry but breaks time-reversal symmetry (TRS). While these properties enabled the prediction of a number of unusual superconducting phases [1,2,15,16], their role in Josephson systems is of particular relevance because Josephson junctions (JJs) form the basis for superconducting electronics and quantum computing [17–31]. In this regard, AMs in single JJs have already proven crucial for inducing spin-polarized Andreev bound states (ABSs) [32–35], anomalous supercurrents [32,34,36–43], and nonreciprocal critical currents [44–50]. These advances show the potential of altermagnetism in single JJs, and naturally make us wonder about the impact of altermagnetism on coherently coupled JJs.

The coherent coupling of JJs has already inspired several theoretical [51–65] and experimental [66–77] efforts. Central to these works is the formation of Andreev molecules due to the hybridization of ABSs when coupling two JJs [51], a phenomenon tunable by the superconducting phase differences across each JJ. Andreev molecules form similarly to how natural atoms bond to form chemical molecules but based on the Andreev and Josephson physics. A unique property of the Andreev molecular regime is that the supercurrent flow across one JJ can be manipulated by the phase difference across the other JJ, enabling the so-called nonlocal Josephson effect (JE) [51]. At present, there already exists experimental evidence of Andreev molecules and of the nonlocal JE, thus supporting coherently coupled JJs for creating fundamental states and intriguing material properties. Despite this progress, however, the research on Andreev molecules and nonlocal JE has mainly focused on superconductor-semiconductor systems, leaving seldom studied the role of the recently discovered altermagnetism.

In this work, we consider three coupled spin-singlet s-wave superconductors with d-wave altermagnetism and demonstrate the formation of spin-polarized Andreev molecules when spin-polarized ABSs of each JJ hybridize across the middle superconductor. Notably, we find that the spin-polarized Andreev molecules enable anomalous phase-biased nonlocal Josephson effects, whereby a phase difference across one junction induces a supercurrent through the other. Depending on the altermagnetic crystal symmetries and strength of altermagnetism, the nonlocal Josephson current develops tunable transitions between 0-, π-, and ϕ_0-junction behaviors. We also show that the nonlocal supercurrents carried by spin-polarized Andreev molecules develop a nonreciprocal behavior, thereby signaling the emergence of a nonlocal Josephson diode effect. We find that the efficiency and polarity of this diode effect exhibit a strong tunability by the type and strength of altermagnetism. The core feature unifying these diverse phenomena is the emergent, spin-polarized nature of the Andreev molecules. Because d-wave altermagnetism spin splits the Fermi surface in a momentum-dependent way while maintaining zero net magnetization, the hybridized Andreev bound states inherit a unique altermagnetic spin polarization. This resulting spin polarization acts as the singular catalyst for the anomalous nonlocal Josephson response, the 0-, π-, and ϕ_0-junction transitions, and the nonlocal Josephson diode

*Contact author: jorge.cayao@physics.uu.se

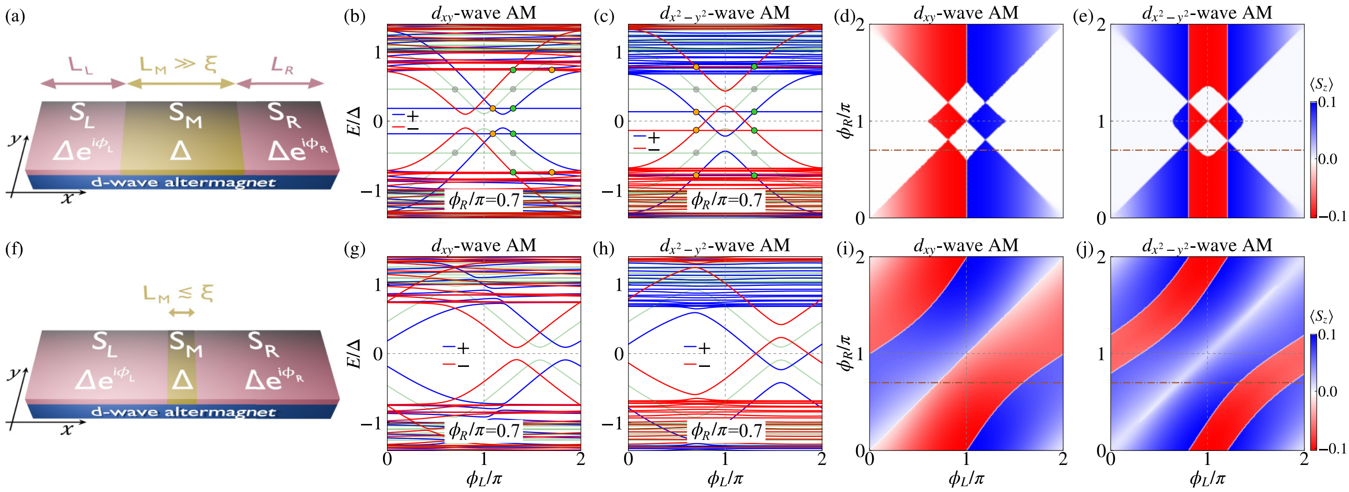

FIG. 1. (a), (f) Sketch of the studied Josephson setup, where three spin-singlet s-wave superconductors denoted by S_α [$\alpha = \mathrm{L, R}$ (pink) and $\alpha = \mathrm{M}$ (gold)] are in contact with a d-wave altermagnet (blue); the superconductors have lengths L_α and pair potentials $\Delta_\alpha = \Delta e^{i\phi_\alpha}$, with $\phi_{\mathrm{M}} = 0$. Panels (a) and (f) correspond to S_{M} with a long ($L_{\mathrm{M}} = 100a \gg \xi$) and a short ($L_{\mathrm{M}} = 2a \lesssim \xi$) length, where ξ is the superconducting coherence length and a is the lattice spacing. Low-energy spectrum as a function of ϕ_{L} at $\phi_{\mathrm{R}} = 0.7\pi$ and $k_y = 0.1\pi$ for (b), (c) $L_{\mathrm{M}} \gg \xi$, and (g), (h) for $L_{\mathrm{M}} \lesssim \xi$. The blue (red) color in panels (b), (c), (g), and (h) indicates that such energy levels belong to the Nambu sector formed by spin-$\uparrow$ electrons (holes) with spin-$\downarrow$ holes (electrons), denoted by "+" ("−"). The light green curves are the energy levels without altermagnetism. The filled yellow and green circles mark the positions where dispersionless levels of the right JJ cross with the dispersive levels of the left JJ in the presence of the AM, while the filled gray circles mark the same but in the absence of the AM. Spin projection along z in the left JJ at $k_y = 0.1\pi$ for (d), (e) $L_{\mathrm{M}} \gg \xi$, and (i), (j) for $L_{\mathrm{M}} \lesssim \xi$. Parameters: $L_{\mathrm{L}} = L_{\mathrm{R}} = 100a$, $\mu = 1.5t$, $\Delta = 0.2t$, $J_1 = 0.1t$, $J_2 = 0.1t$, and $\phi_{\mathrm{M}} = 0$.

effect alike. Our work establishes the interplay between altermagnetism and coherently coupled JJs as an outstanding ground for designing nonlocal Josephson phases with spintronic functionalities.

The remainder of this work is organized as follows. In Sec. II, we present the model of coherently coupled Josephson junctions with d-wave altermagnetism. In Sec. III, we demonstrate the emergence of spin-polarized Andreev molecules, while in Secs. IV and V we discuss their impact on the nonlocal Josephson effect and the nonlocal Josephson diode effect, respectively. In Sec. VI, we present our conclusions.

II. COUPLED JOSEPHSON JUNCTIONS WITH *d*-WAVE ALTERMAGNETISM

We consider the coherent coupling of two JJs with d-wave altermagnetism, where two spin-singlet s-wave superconductors are coupled through a spin-singlet s-wave superconductor [Figs. 1(a) and 1(f)]. The coupled JJs are assumed to be finite along x and periodic along the y, and modeled by

$$\mathcal{H}_{k_y}(\phi_{\mathrm{L}}, \phi_{\mathrm{M}}, \phi_{\mathrm{R}}) = \sum_\alpha H_{k_y}(\phi_\alpha) + H_{\mathrm{LM}} + H_{\mathrm{MR}}, \quad (1)$$

where

$$H_{k_y}(\phi_\alpha) = \sum_i c_i^\dagger h_{ii}(k_y) c_i + \sum_{\langle i,j \rangle} c_i^\dagger v_{ij}(k_y) c_j + \sum_i \Delta_\alpha (c^\dagger_{i_\alpha,\uparrow} c^\dagger_{i_\alpha,\downarrow} - c^\dagger_{i_\alpha,\downarrow} c^\dagger_{i_\alpha,\uparrow}) + \mathrm{H.c.} \quad (2)$$

describes the left (L), middle (M), and right (R) superconductor ($\alpha = \mathrm{L, M, R}$) with d-wave altermagnetism. Here, $c_i = (c_{i,\uparrow}, c_{i,\downarrow})^{\mathrm{T}}$, where $c_{i,\uparrow}$ annihilates an electronic state with spin $\sigma = \uparrow, \downarrow$ at i. Moreover, $h_{ii}(k_y) = [-\mu + 4t - 2t\cos k_y]\sigma_0 - J_2 \cos k_y \sigma_z$ and $v_{ij}(k_y) = -t\sigma_0 - iJ_1 \sin k_y \sigma_z + (J_2/2)\sigma_z$ correspond to on-site and nearest-neighbor terms, which are block diagonal in spin space, σ_i are the spin Pauli matrices, t denotes the hopping strength, μ is the chemical potential, while J_1 and J_2 represent the strength of the d_{xy}- and $d_{x^2-y^2}$-wave altermagnetism. Furthermore, $\Delta_\alpha = \Delta e^{i\phi_\alpha}$ is the pair potential in α superconductor; by gauge symmetry [65], we set $\phi_{\mathrm{M}} = 0$ and keep $\phi_{\mathrm{L,R}} \neq 0$ characterizing the superconducting phase differences across the left and right JJs. We treat ϕ_{L} and ϕ_{R} as independent control parameters, as in multiterminal Josephson structures [51,78], where the superconducting phase differences are biased independently by threading magnetic fluxes through superconducting loops attached to the superconductors. We assume an infinitely wide junction geometry with perfect translational invariance along the y axis, rendering k_y a conserved quantum number [37,38,79]. This approximation remains highly accurate because any phase-biasing circuitry or loop boundaries are localized at the macroscopic edges, far from the mesoscopic transport channel. Furthermore, since the altermagnetic spin splitting occurs at zero external magnetic field [1], the local Hamiltonian remains strictly uniform along the interface. The term $H_{\mathrm{LM(MR)}}$ couples the left and middle (middle and right) superconductors, having nonzero values only between the sites adjacent to the interfaces. Next, we denote $\mathcal{H}_{k_y}(\phi_{\mathrm{L}}, \phi_{\mathrm{R}}) \equiv \mathcal{H}_{k_y}(\phi_{\mathrm{L}}, \phi_{\mathrm{M}} = 0, \phi_{\mathrm{R}})$.

Before going further, we discuss the symmetries of the JJ setup in Eq. (1). Without the AM, the JJ Hamiltonian preserves global time-reversal symmetry,

$\mathcal{TH}(\phi_L, \phi_R)\mathcal{T}^{-1} = \mathcal{H}(-\phi_L, -\phi_R)$, but local TRS can be broken, $\mathcal{TH}(\phi_L, \phi_R)\mathcal{T}^{-1} \neq \mathcal{H}(-\phi_L, \phi_R)$, where $\mathcal{T}$ denotes the time-reversal operator. In the presence of an AM, global TRS is broken. In addition, in the presence and absence of AM, the JJ intrinsically breaks local spatial inversion, $\mathcal{IH}(\phi_L, \phi_R)\mathcal{I}^{-1} \neq \mathcal{H}(-\phi_L, \phi_R)$, with $\mathcal{I}$ the inversion operator. Thus, breaking local time-reversal and local inversion symmetries is very likely to lead to unusual ABSs and supercurrents; in fact, the simultaneous breaking of these symmetries satisfies the necessary conditions for the Josephson diode effect [80–90], suggesting that our JJ in Eq. (1) can host intriguing Josephson physics.

III. SPIN-POLARIZED ANDREEV MOLECULES

We begin by inspecting the role of the superconducting phase differences $\phi_{L,R}$ in the low-energy spectrum of our coupled JJs with altermagnetism [Eq. (1)]. For this reason, Figs. 1(b) and 1(c) show the low-energy spectrum as a function of ϕ_L with $d_{x^2-y^2}$- and d_{xy}-wave altermagnetism; in both cases, $\phi_R = 0.7\pi$, $k_y = 0.1\pi$ for a middle superconductor longer than the superconducting coherence length ξ ($L_M \gg \xi$). To contrast this regime, Figs. 1(g) and 1(h) show the low-energy spectrum for a short middle superconductor ($L_M \lesssim \xi$). These short and long middle superconductor regimes capture the weak and strong couplings between JJs. To complement the analysis in these two regimes, Figs. 1(d), 1(e), 1(i), and 1(j) show the spin polarization $\langle S_z\rangle$ in the left JJ for the first positive ABS. In the absence of altermagnetism, the left (right) JJ hosts four spin-degenerate ABSs that depend on $\phi_{L,R}$ and L_M, with a 2π-periodic energy spectrum that is symmetric about $\phi_L = \pi$ [see light green curves in Figs. 1(b), 1(c), 1(g), and 1(h)]. For $L_M \gg \xi$, the left and right JJs behave as independent [Figs. 1(b) and 1(c)]: The ABSs of the left JJ exhibit a strong dependence on ϕ_L, while the ABSs of the right JJ remain dispersionless and intersect the ABSs of the left JJ at $\phi_R = \phi_L$, as indicated by the gray circles in Fig. 1(b). In contrast, for $L_M \lesssim \xi$ [Figs. 1(g) and 1(h)], the ABSs of both junctions hybridize, leaving only a single pair of hybridized ABSs that strongly disperses with $\phi_{L,R}$ and is asymmetric with respect to $\phi_L = \pi$. The dependence of the hybridized ABSs on L_M resembles an interatomic potential describing molecular formation, giving rise to the so-called Andreev molecules [51]; see Fig. 4 in Appendix A for the molecular energy dependence on L_M and Fig. 5 in Appendix B for the real-space wave function hybridization.

With altermagnetism, the low-energy spectrum develops interesting changes in short and long middle superconductors [see Figs. 1(b), 1(c), 1(g), and 1(h)]. First, a finite amount of altermagnetism makes ABSs to split in spin, giving rise to spin-polarized ABSs with a behavior that strongly depends on the ratio between L_M and ξ as well as on the type of altermagnetism and $\phi_{L,R}$. For $L_M \gg \xi$, only the spin-polarized ABSs of the left JJ disperse with ϕ_L, while the spin-polarized ABSs of the right JJ remain dispersionless and intersect the ABSs of the left JJ at $\phi_R = \phi_L$; owing to the 2π periodicity of the spectrum, a similar intersection occurs at $\phi_R = 2\pi - \phi_L$ [see Figs. 1(b) and 1(c) and yellow/green circles]. The fact that ABSs of the left JJ disperse only with ϕ_L and those of the right JJ remain dispersionless occurs because the left and right JJs are weakly coupled due to $L_M \gg \xi$. Interestingly, while d_{xy}-wave altermagnetism splits ABSs shifting them to distinct minima above and below $\phi_L = \pi$, $d_{x^2-y^2}$-wave altermagnetism splits ABSs to higher and lower energies but maintaining the same minimum at $\phi = \pi$. This dependence in $d_{x^2-y^2}$-wave AMs makes ABSs to reach and cross zero energy, as in Fig. 1(c). Moreover, the finite size of the setup naturally induces a quasicontinuum, where, depending on the strength and type of altermagnetism, the spin-polarized ABSs can leak and/or touch the gap edges; for instance, under d_{xy}-wave altermagnetism, ABSs with distinct spin polarization touch the gap edges at $\phi_L = 0, 2\pi$, while ABSs of the same polarization reach the gap edges at $\phi_L = 0, 2\pi$ with $d_{x^2-y^2}$-wave altermagnetism. Despite these differences between altermagnetic symmetries at $L_M \gg \xi$, the energy spectrum is symmetric about $\phi_L = \pi$ for any ϕ_R.

When the middle superconductor is very short ($L_M \lesssim \xi$), the spin-polarized ABSs of the left and right JJs undergo a strong hybridization that gives rise to spin-polarized Andreev molecules [see Figs. 1(g) and 1(h)]. These spin-polarized Andreev molecules now constitute the subgap states of the strongly coupled JJs, and are, therefore, extremely sensible to variations of $\phi_{L,R}$. In fact, d_{xy}-wave altermagnetism splits the hybridized ABSs into spin-polarized Andreev molecules along ϕ_L, developing minima below and above ϕ_L^* [Fig. 1(g)], with ϕ_L^* being the value of ϕ_L at which the Andreev molecule has a minimum without altermagnetism. This behavior enables JJs with d_{xy}-wave AMs to host Andreev molecules with distinct polarizations at the same energies with a behavior that is asymmetric about $\phi_L = \pi$. For $d_{x^2-y^2}$-wave altermagnetism, the spin-polarized Andreev molecules are asymmetric about $\phi_L = \pi$ and shifted in energy at ϕ_L^*; depending on the altermagnetic strength, they can reach and cross zero energy [see Fig. 1(h)]. This leaves spin-polarized Andreev molecules with distinct spin polarizations crossing zero energy and at higher energies. The zero-energy crossings of the Andreev molecules are robust unless fields that couple distinct spins are applied. It is worth noting that the hybridized ABSs also leak into the quasicontinuum, but with subtle differences in each altermagnetic symmetry: The quasicontinuum of the JJ with d_{xy}-wave altermagnetism is composed of mixed levels having the same and distinct polarizations, which implies that the spin-polarized Andreev molecule leaking into such quasicontinuum also hybridizes with the quasicontinuum levels of the same polarization [Fig. 1(g)]. In contrast, the quasicontinuum of the JJ with $d_{x^2-y^2}$-wave altermagnetism contains spin-polarized subsets at distinct energies, which ensures that the spin-polarized Andreev molecules leaking into the quasicontinuum do not hybridize with the quasicontinuum levels [Fig. 1(h)].

The spin-polarized nature is also supported by the behavior of the spin polarization $\langle S_z\rangle$, which we obtain in the left JJ and show in Figs. 1(d), 1(e), 1(i), and 1(j) as a function of $\phi_{L,R}$ at $k_y \neq 0$. Figures 1(d) and 1(e) show that $\langle S_z\rangle$ for $L_M \gg \xi$ behaves as an odd function of ϕ_L for the d_{xy}-wave AMs ($\langle S_z(\phi_L)\rangle = -\langle S_z(-\phi_L)\rangle$), whereas it behaves as an even function for the $d_{x^2-y^2}$-wave AMs ($\langle S_z(\phi_L)\rangle = \langle S_z(-\phi_L)\rangle$). By close inspection, the profile of $\langle S_z\rangle$ aligns well with the

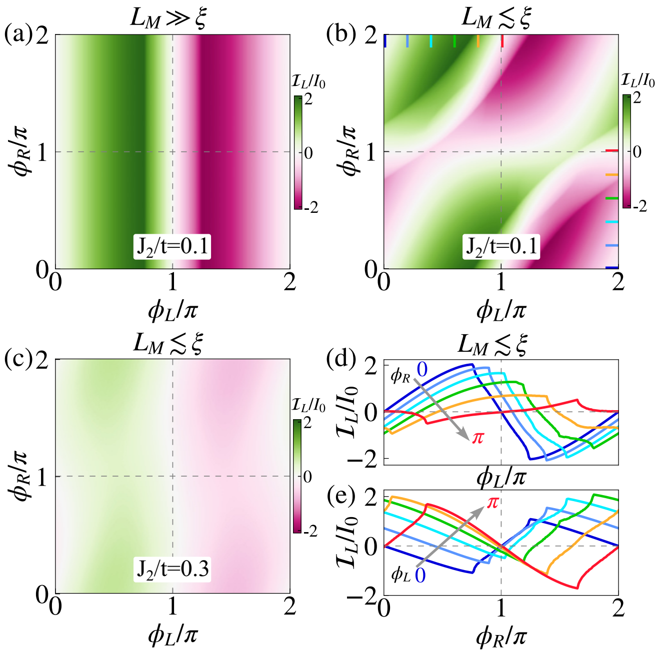

FIG. 2. Josephson current $\mathcal{I}_{\rm L}$ across the left JJ as a function of $\phi_{\rm L,R}$ in the presence of $d_{x^2-y^2}$-wave altermagnetism. $\mathcal{I}_{\rm L}$ for (a) $L_{\rm M} = 100a \gg \xi$ and $J_2/t = 0.1$, and (b), (c) for $L_{\rm M} = 2a \lesssim \xi$ and $J_2/t = \{0.1, 0.3\}$. (d), (e) Line cuts of $\mathcal{I}_{\rm L}$ in panel (b) as a function of $\phi_{\rm L(R)}$ at distinct $\phi_{\rm R(L)}$ in steps of 0.2π marked by color bars in panel (b). Rest of parameters are same in Fig. 1.

spin-polarized nature of the ABSs shown in Figs. 1(b) and 1(c) [see dash-dotted line in Figs. 1(d) and 1(e)]. In contrast, for $L_{\rm M} \lesssim \xi$, $\langle S_z \rangle$ acquires a distinct behavior that reflects opposite spin polarization along $\phi_{\rm L} = \phi_{\rm R}$: This implies that $\langle S_z(\phi_{\rm L}, \phi_{\rm R})\rangle = \pm\langle S_z(-\phi_{\rm L}, -\phi_{\rm R})\rangle$ for the JJs with d_{xy}- and $d_{x^2-y^2}$-wave altermagnetism, reflecting the key role of $\phi_{\rm R}$. Still, $\langle S_z \rangle$ determines the spin polarization of the emergent Andreev molecules. Thus, Figs. 1(d), 1(e), 1(i), and 1(j) not only support the spin-polarized nature of Andreev molecules but also demonstrate the nonlocal phase control of spin polarization in coupled JJs.

IV. ANOMALOUS NONLOCAL JOSEPHSON CURRENTS

Having shown the emergence of spin-polarized Andreev molecules, we now focus on the phase-biased Josephson current flowing across the left JJ, obtained for each k_y as $I_{\rm L}(k_y, \phi_{\rm L}, \phi_{\rm R}) = (e/\hbar)\sum_{E_n<0} \partial E_n(k_y, \phi_{\rm L}, \phi_{\rm R})/\partial\phi_{\rm L}$ [31,91,92]; this provides a way to pinpoint the contributions of distinct energy levels [93–99]. The total Josephson current flowing across the left JJ is then found as $\mathcal{I}_{\rm L}(\phi_{\rm L}, \phi_{\rm R}) = \int I_{\rm L}(k_y, \phi_{\rm L}, \phi_{\rm R}) dk_y$, which accounts for the weight of all transverse channels [1]. With this, in Fig. 2 we show $\mathcal{I}_{\rm L}(\phi_{\rm L}, \phi_{\rm R})$ as a function of $\phi_{\rm L,R}$ in the presence of $d_{x^2-y^2}$-wave altermagnetism for long ($L_{\rm M} \gg \xi$) and short ($L_{\rm M} \lesssim \xi$) middle superconductors; for d_{xy}-wave altermagnetism, see Fig. 6 in Appendix C. When $L_{\rm M} \gg \xi$, the current $\mathcal{I}_{\rm L}(\phi_{\rm L}, \phi_{\rm R})$ is an odd function and 2π-periodic with respect to $\phi_{\rm L}$ but insensitive to $\phi_{\rm R}$, namely, $\mathcal{I}_{\rm L}(\phi_{\rm L}, \phi_{\rm R}) = -\mathcal{I}_{\rm L}(-\phi_{\rm L}, \phi_{\rm R})$ and $\mathcal{I}_{\rm L}(2\pi + \phi_{\rm L}, \phi_{\rm R}) = \mathcal{I}_{\rm L}(\phi_{\rm L}, \phi_{\rm R})$ [Fig. 2(a)]; these dependences also appear in regular JJs [100]. This is an expected behavior consistent with the ABSs in Fig. 1(c) since the left and right JJs are effectively uncoupled and the spin-polarized ABSs of the right JJ along with $\phi_{\rm R}$ do not affect the properties of the left JJ.

When $L_{\rm M} \lesssim \xi$, the hybridization of spin-polarized ABSs that leads to spin-polarized Andreev molecules strongly affects the phase dependence of $\mathcal{I}_{\rm L}(\phi_L, \phi_R)$ [see Figs. 2(b)–2(d)]. In particular, $\mathcal{I}_{\rm L}(\phi_L, \phi_R)$ is now strongly dependent on $\phi_{\rm R}$, developing negative/positive values for $\phi_{\rm L} < \pi$ and $\phi_{\rm L} > \pi$, which depend on the strength of altermagnetism and are achieved after passing through zero values in both types of the studied AMs [see Figs. 2(b), 2(c), 6(b), and 6(c)]. Interestingly, $\mathcal{I}_{\rm L}(\phi_{\rm L}, \phi_{\rm R}) \neq 0$ at $\phi_{\rm L} = n\pi$, with $n \in \mathbb{Z}$, and its oddness is now reflected by the simultaneous action of both phases $\phi_{\rm L,R}$ as $\mathcal{I}_{\rm L}(\phi_L, \phi_R) = -\mathcal{I}_{\rm L}(-\phi_L, -\phi_R)$; this occurs in $d_{x^2-y^2}$- and d_{xy}-wave altermagnetism [see Figs. 2(b), 2(c), 6(b), and 6(c)]. As consequence of these properties is that the current flowing across the left junction develops ϕ_0- and π-junction behaviors, as a function of either$\phi_{\rm L}$ or $\phi_{\rm R}$ [see Figs. 2(d) and 2(e)]. It is thus possible to have $\mathcal{I}_{\rm L}(\phi_{\rm L} = 0, \phi_{\rm R} \neq 0) \neq 0$ or $\mathcal{I}_{\rm L}(\phi_{\rm L} + \pi, \phi_{\rm R}) = -\mathcal{I}_{\rm L}(\phi_{\rm L}, \phi_{\rm R})$ for a ϕ_{L0} junction or π junction, respectively. JJs with d_{xy}-wave altermagnetism can also host similar junction profiles [see Figs. 6(d) and 6(e)].

The strong dependence of the current flowing across the left JJ by varying the phase difference across the right JJ signals the emergence of the nonlocal Josephson effect. This effect in the left JJ is entirely determined by the spin-polarized Andreev molecules shown in Figs. 1(g) and 1(h), with current signals that can be directly tied to the respective energy branch. For instance, the large values of the current for $\phi_{\rm L} \in (0, \pi)$ and $\phi_{\rm L} \in (\pi, 2\pi)$ in JJs with $d_{x^2-y^2}$-wave altermagnetism are predominantly carried by Andreev molecules of one type of spin polarization within the gap, while outside it the opposite polarization also contributes [Fig. 1(h)]. In contrast, the arc surface region with smaller current intensities for $\phi_{\rm L} \in (\pi, 2\pi)$ corresponds to a regime where the Andreev molecules with distinct polarizations cross zero energy [Fig. 1(h)], leaving Andreev molecules with the same polarization but opposite contribution that end up canceling out; thus, the values of the current in this case are dominated by the quasicontinuum. In a similar way, one can identify the contribution of spin-polarized Andreev molecules on the nonlocal Josephson effect in coupled JJs with d_{xy}-wave altermagnetism [see Figs. 6(b) and 6(c) in Appendix C]. We can therefore conclude that the formation of spin-polarized Andreev molecules enables the emergence of a nonlocal Josephson effect determining supercurrents with anomalous profiles.

V. NONLOCAL JOSEPHSON DIODE EFFECT

The behavior of the nonlocal Josephson current $\mathcal{I}_{\rm L}(\phi_{\rm L}, \phi_{\rm R})$ also reveals its nonreciprocity since the maximum and minimum currents are not equal, $\mathcal{I}^{+}_{\rm cL}(\phi_{\rm R}) \neq \mathcal{I}^{-}_{\rm cL}(\phi_{\rm R})$, where $\mathcal{I}^{\pm}_{\rm cL}(\phi_{\rm R}) = \max_{\phi_{\rm L}}[\pm\mathcal{I}_{\rm L}(\phi_L, \phi_{\rm R})]$. Using these definitions, in Fig. 3(a) we show $\mathcal{I}^{\pm}_{\rm cL}(\phi_{\rm R})$ as a function of J_2 and $\phi_{\rm R}$ for a very short middle region $L_{\rm M} = 2a$ in the presence of $d_{x^2-y^2}$-wave altermagnetism. Figure 3(a) shows that $\mathcal{I}^{+}_{\rm cL}(\phi_{\rm R}) \neq \mathcal{I}^{-}_{\rm cL}(\phi_{\rm R})$

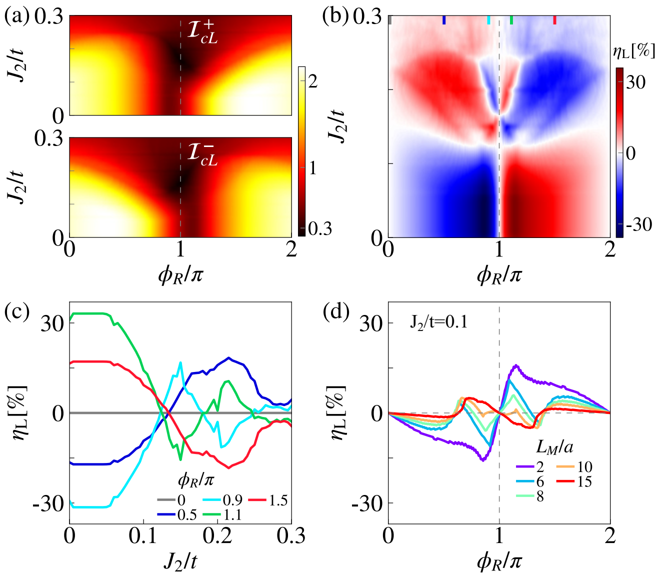

FIG. 3. (a) Critical currents $\mathcal{I}_{\rm cL}^{\pm}$ as a function of $\phi_{\rm R}$ and J_2 under $d_{x^2-y^2}$-wave altermagnetism. (b) Quality factor $\eta_{\rm L}$ as a function of J_2 and $\phi_{\rm R}$. (c), (d) Line cuts of panel (b) for distinct values of J_2 and $\phi_{\rm R}$. The values of $\phi_{\rm R}$ for the line cuts in panel (c) are marked by color bars in panel (b). Parameters: $L_{\rm M}=2a$ and the rest is the same as in Fig. 1.

for any $\phi_{\rm R}$, except $\phi_{\rm R}=n\pi$, with $n\in\mathbb{Z}$. The nonreciprocity in the nonlocal critical currents signals the emergence of the nonlocal Josephson diode effect. While $\mathcal{I}_{\rm cL}^{\pm}(\phi_{\rm R})$ remains sizable for J_2 below Δ, strong altermagnetic strengths tend to reduce the critical currents; in JJs with $d_{x^2-y^2}$-wave altermagnetism [Fig. 3(a)], the currents support stronger values of altermagnetic fields than in JJs with d_{xy}-wave AMs [see Appendix D and Fig. 7(a)].

To assess the efficiency of the nonlocal Josephson diode effect, we obtain its quality factor as $\eta_{\rm L}(\phi_{\rm R})=[\mathcal{I}_{\rm cL}^{+}(\phi_{\rm R})-\mathcal{I}_{\rm cL}(\phi_{\rm R})^{-}]/[\mathcal{I}_{\rm cL}^{+}(\phi_{\rm R})+\mathcal{I}_{\rm cL}^{-}(\phi_{\rm R})]$ and show it in Fig. 3(b) as a function of J_2 and $\phi_{\rm R}$ for JJs with $d_{x^2-y^2}$-wave altermagnetism, while in Fig. 7(b) for thed_{xy}-wave AM case. The first observation is that $\eta_{\rm L}$ strongly depends on $\phi_{\rm R}$ as well as on the strength and type of altermagnetism. For $\phi_{\rm R}=n\pi$, with $n\in\mathbb{Z}$, the quality factor vanishes since $\mathcal{I}_{\rm cL}^{+}=\mathcal{I}_{\rm cL}^{-}$; in this case, the Andreev spectrum is symmetric around $\phi_{\rm L}=\pi$. Away from these phase values, $\eta_{\rm L}$ reach efficiencies on the order of 30% and notably develops an odd function dependence with $\phi_{\rm R}$ as a clear manifestation of the nonlocal Josephson effect; this also means that the diode's polarity ${\rm sgn}(\eta_{\rm L})$ can be controlled nonlocally by $\phi_{\rm R}$ [see Figs. 3(c) and. 7(c)]. Furthermore, the diode's polarity can be controlled by the strength of altermagnetism, as demonstrated in Figs. 3(c), 3(d), 7(c), and 7(d) at fixed $\phi_{\rm R}$. Under $d_{x^2-y^2}$-wave altermagnetism, changing the diode's polarity requires slightly stronger altermagnetic fields than under d_{xy}-wave altermagnetism but the former supports larger efficiencies at large fields. Nevertheless, in both types of AMs, reaching measurable nonlocal Josephson diode efficiencies requires the presence of spin-polarized Andreev molecules, which is only attained for short middle superconductors, as demonstrated in Figs. 3(d) and 7(d).

VI. CONCLUSIONS

In conclusion, we have demonstrated the formation of spin-polarized Andreev molecules in weakly coupled Josephson junctions with zero net magnetization by utilizing altermagnetism. We showed that these spin-polarized Andreev molecules give rise to phase-biased nonlocal Josephson currents capable of developing ϕ_0- and π-junction behaviors, which are tunable by the type and strength of altermagnetism. Moreover, we found that these nonlocal Josephson currents exhibit nonreciprocal critical currents, originating a nonlocal Josephson diode effect whose polarity is controllable nonlocally by the superconducting phase difference across the right Josephson junction as well as by the strength of altermagnetism. These predictions are applicable to higher angular momentum altermagnets, such as g and i wave, and offer a very likely nonlocal phase control of recently reported altermagnet-induced phenomena, such as exotic Cooper pairs [15,101–113] and flat bands [114–116]. We emphasize that the diverse phenomena reported here are not independent effects, but rather distinct macroscopic manifestations of a single microscopic origin. By combining a vanishing net magnetization with momentum-dependent spin splitting, altermagnetism fundamentally spin polarizes the hybridized Andreev molecules. This resulting molecular spectrum serves as the unified engine driving the anomalous nonlocal currents, the junction-character transitions, and the tunable diode polarity. Our results position altermagnetism as a foundational building block for engineering spin-polarized Andreev molecules and achieving anomalous Josephson states with nonlocal spintronic functionalities.

ACKNOWLEDGMENTS

We acknowledge financial support from the Göran Gustafsson Foundation (Grant No. 2216), from the Swedish Research Council (Vetenskapsrådet Grant No. 2021-04121), and from the Olle Engkvist Foundation (Grant No. 243-1026). The computations were enabled by resources provided by the National Academic Infrastructure for Supercomputing in Sweden (NAISS), partially funded by the Swedish Research Council through Grant Agreement No. 2022-06725.

DATA AVAILABILITY

There are no publicly available research data or software supporting this manuscript. Requests for further information or data should be sent to the authors.

APPENDIX A: MOLECULAR BEHAVIOR OF THE HYBRIDIZED ANDREEV STATES

The molecular nature of the spin-polarized ABSs can be directly seen in the dependence of the energy levels on $L_{\rm M}$, presented in Fig. 4 at $\phi_{\rm L}=0.7\pi=\phi_{\rm R}$ and $\phi_{\rm L}=1.3\pi\neq\phi_{\rm R}$ for altermagnetic strengths corresponding to Fig. 1. Without AMs, the energy levels are spin degenerate but already here the levels develop an interesting behavior with $L_{\rm M}$ [see Fig. 4(a)]: At long $L_{\rm M}$, each JJ hosts ABSs that are degenerate but begin to split at $L_{\rm M}\sim 50a$, followed by a behavior that depends on $\phi_{\rm L,R}$. For $\phi_{\rm L}=1.3\pi\neq\phi_{\rm R}$, the energy levels below

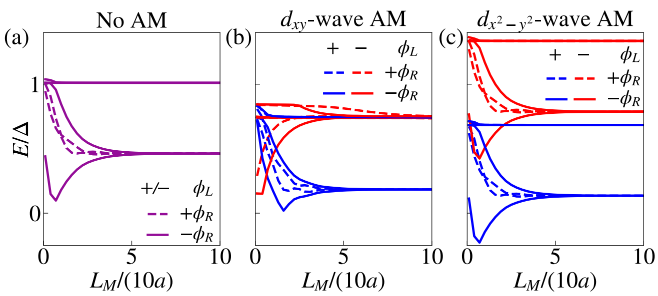

FIG. 4. Lowest four positive levels of each $\pm$ sector as a function of $L_{\rm M}$ in the absence [panel (a)] and presence [panels (b), (c)] of altermagnetism at $\phi_{\rm R} = 0.7\pi$ and $k_y = 0.1\pi$. The dashed and solid curves correspond to $\phi_{\rm L} = 0.7\pi = \phi_{\rm R}$ and $\phi_{\rm L} = 1.3\pi = -\phi_{\rm R}$, respectively. Parameters: $J_{1,2} = 0$ in panel (a), $J_1 = 0.1t$ and $J_2 = 0$ in panel (b), $J_1 = 0$ and $J_2 = 0.1t$ in panel (c), and the rest as in Fig. 1.

$L_{\rm M} \sim 50a$ form bonding and antibonding molecular states, with a clear minimum and an overall energy dependence that resembles the interatomic potential describing molecular formation [Fig. 4(a)]. For $\phi_{\rm L} = 0.7\pi = \phi_{\rm R}$, the splitting between ABSs induced by the hybridization is weaker below $L_{\rm M} \sim 50a$, ultimately pushing both levels into the quasicontinuum. Interestingly, in the presence of altermagnetism, ABSs are split in spin and, interestingly, such spin-polarized ABSs still develop the molecular formation profile for $\phi_{\rm L} = 1.3\pi \neq \phi_{\rm R}$ and in both types of altermagnetism [see Figs. 4(b) and 4(c)]. This demonstrates the emergence of spin-polarized Andreev molecules.

APPENDIX B: LOCALIZATION OF ANDREEV MOLECULES

The hybridization of spin-polarized ABSs in the JJ setup of Fig. 1(a) is due to the reduced length of the middle superconductor, which leads to a strong coupling between left and right JJs. To see the real-space behavior of such hybridization, Fig. 5 shows the space dependence of the wave function probability density of the first positive state for $L_{\rm M} = 100a$ and $L_{\rm M} = 2a$ for distinct $\phi_{\rm L,R}$. When $L_{\rm M} = 100a$, the coupling between left and right JJs is very weak, such that the ABSs localized at each JJ do not hybridize [Fig. 5(a)]: As seen, the

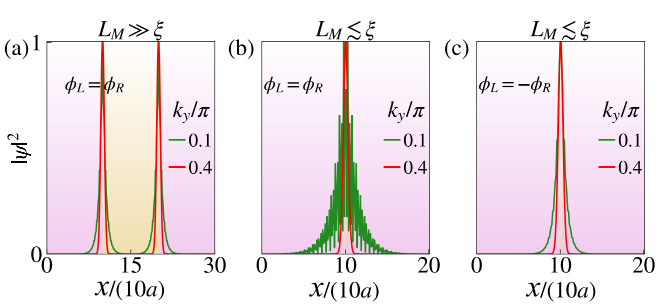

FIG. 5. Wave function probability density of the first positive state for a JJ with $d_{x^2-y^2}$-wave altermagnetism as a function of space for $L_M = 100a$ [panel (a)] and $L_M = 2a$ [panels (b), (c)], in both cases with $\phi_{\rm R} = 0.7\pi$. The green and the red curves indicate two different values of k_y. Parameters: $J_1 = 0$ and $J_2 = 0.1t$; the rest is the same as in Fig. 1.

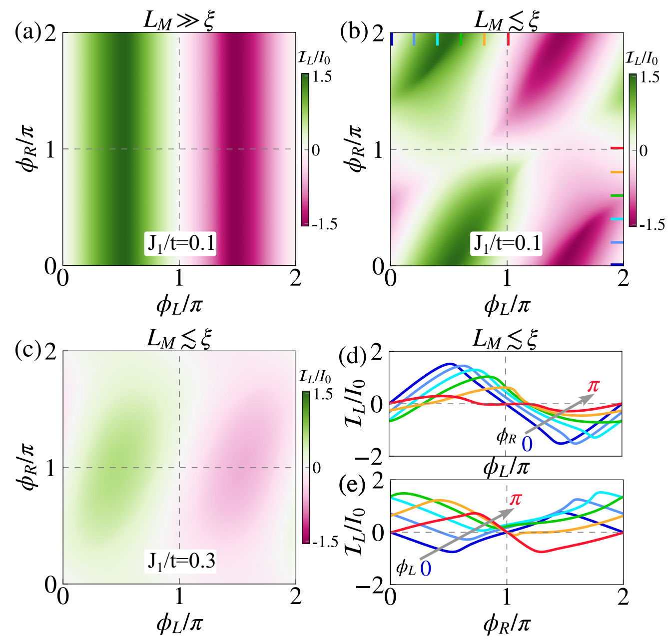

FIG. 6. The Josephson current $\mathcal{I}_{\rm L}$ across the left JJ as a function of $\phi_{\rm L,R}$ in the presence of d_{xy}-wave altermagnetism. $\mathcal{I}_{\rm L}$ for (a) $L_{\rm M} = 100a \gg \xi$ and $J_1/t = 0.1$, and (b), (c) for $L_{\rm M} = 2a \lesssim \xi$ and $J_1/t = \{0.1, 0.3\}$. (d), (e) Line cuts of $\mathcal{I}_{\rm L}$ in panel (b) as a function of $\phi_{\rm L(R)}$ at distinct $\phi_{\rm R(L)}$ in steps of 0.2π marked by color bars in panel (b). Parameters are same in Fig. 1.

ABSs are strongly localized at each JJ, with their wave functions decaying toward the bulk of the middle superconductor that depends on k_y but without developing any spatial overlap. In contrast, for $L_{\rm M} = 2a$, the wave functions of the ABSs of the left and right JJs strongly hybridize, with a profile that resembles that of an ABS localized at a single interface. The wave function profile of this spin-polarized Andreev molecule depends on k_y and $\phi_{\rm L,R}$, which can influence the decay itself and its oscillations.

APPENDIX C: NONLOCAL JOSEPHSON CURRENTS IN JUNCTIONS WITH d_{xy}-WAVE ALTERMAGNETISM

In the case of d_{xy}-wave altermagnetism, the total Josephson current flowing across the left JJ, $\mathcal{I}_{\rm L}(\phi_{\rm L}, \phi_{\rm R})$, is presented in Figs. 6(a) and 6(b) as a function of $\phi_{\rm L,R}$ for long ($L_{\rm M} \gg \xi$) and short ($L_{\rm M} \lesssim \xi$) middle superconductors at $J_1/t = 0.1$. Figure 6(c) show $\mathcal{I}_{\rm L}(\phi_{\rm L}, \phi_{\rm R})$ versus $\phi_{\rm L,R}$ for $J_1/t = 0.3$, while Figs. 6(d) and 6(e) shows line cuts of Fig. 6(b) as a function of $\phi_{\rm L,R}$ at distinct $\phi_{\rm R,L}$. For $L_{\rm M} \gg \xi$, Fig. 6(a) reveals that $\mathcal{I}_{\rm L}(\phi_{\rm L}, \phi_{\rm R})$ is an odd function of $\phi_{\rm R}$ but independent of $\phi_{\rm R}$; this is because the left and right JJs are effectively uncoupled (very weakly coupled) and the spin-polarized ABSs in each JJ do not hybridize. When $L_{\rm M} \lesssim \xi$, $\mathcal{I}_{\rm L}(\phi_{\rm L}, \phi_{\rm R})$ exhibits large intensities that strongly depend on both $\phi_{\rm L,R}$ and J_1 [see Figs. 6(b)–6(d)]. First of all, $\mathcal{I}_{\rm L}(\phi_{\rm L}, \phi_{\rm R})$ is an odd function under both $\phi_{\rm L,R}$ and develops nonzero values at $\phi_{\rm L} = n\pi$ for $\phi_{\rm R} \neq n\pi$ [Fig. 6(b)], similar to JJs with $d_{x^2-y^2}$-wave altermagnetism shown in Figs. 2(b), 2(d), and 2(e). As a result, the current across the left JJ can develop $\phi_{\rm L0}$-junction behavior as a function of $\phi_{\rm L,R}$ but π behavior only as a function of

ϕ_R [Figs. 2(b), 2(d), and 2(e)], hence establishing similarities and differences with respect to JJs with $d_{x^2-y^2}$-wave altermagnetism. The different behaviors can be controlled by the strength of d_{xy}-wave altermagnetism [Fig. 2(c)].

The intriguing behavior of the anomalous Josephson current $\mathcal{I}_L(\phi_L, \phi_R)$ discussed above can be directly traced back to the behavior of the spin-polarized Andreev molecules shown in Fig. 1(g). For instance, for $\phi_R = 0.7\pi$ in Fig. 1(g), the Andreev molecules inside the gap with positive spin polarization produce a negative supercurrent roughly below $\phi_L < 0.7$, while above such a phase, the Andreev molecule with opposite polarization dominates and gives a positive supercurrent [Fig. 6(b)]; this explains the transition from a red to green color in the intensities of the current in Fig. 6(b) [see also region between orange and green horizontal markers in Fig. 6(b)]. The absence of a π-junction behavior as a function of ϕ_L can also be explained with the behavior of the Andreev molecules: Andreev molecules with both polarizations always share the contribution within the gap and $\phi_L \in (0, 2\pi)$ since d_{xy}-wave altermagnetism shifts the subgap levels only in ϕ_L. This makes it challenging to accommodate a single Andreev molecule giving a negative current for JJs with d_{xy}-wave altermagnetism. This is different from what occurs in $d_{x^2-y^2}$-wave altermagnetism [Figs. 2(b) and 2(d)] since therein the altermagnetic field shifts the energy levels in energy, which can leave a single Andreev molecule with a phase dependence supporting a π junction. In sum, the nonlocal Josephson currents across the left JJ under d_{xy}-wave altermagnetism can develop ϕ_{L0}- and π-junction behaviors controlled by the superconducting phases and altermagnetic strength.

APPENDIX D: NONLOCAL JOSEPHSON DIODE EFFECT IN JUNCTIONS WITH d_{xy}-WAVE ALTERMAGNETISM

The anomalous nonlocal Josephson currents flowing across the left junction of Fig. 6 also exhibit regimes with distinct critical currents $\mathcal{I}_{cL}^+(\phi_R) \neq \mathcal{I}_{cL}^-(\phi_R)$, hence leading to a nonlocal Josephson diode effect under d_{xy}-wave altermagnetism characterized by a nonzero quality factor $\eta_L(\phi_R) \neq 0$. To understand this behavior, in Figs. 7(a) and 7(b) we present $\mathcal{I}_{cL}^{\pm}(\phi_R)$ and $\eta_L(\phi_R)$ as functions of ϕ_R and J_1 for a short middle superconductor ($L_M \lesssim \xi$); in Figs. 7(c) and 7(d), we further show $\eta_L(\phi_R)$ as a function of J_1 for distinct ϕ_R and as a function of ϕ_R for different values of L_M. First, the critical currents $\mathcal{I}_{cL}^{\pm}(\phi_R)$ exhibit values that do not follow the same dependence as a function of ϕ_R and J_1, and with a particular asymmetric profile about $\phi_R = \pi$ [see Fig. 7(a)]. By acquiring distinct values, the critical currents become nonreciprocal and signal the emergence of a nonlocal Josephson diode effect in coupled JJs with d_{xy}-wave altermagnetism. This diode effect is characterized by a finite quality factor η_L in Fig. 7(b), which acquires an odd function dependence in ϕ_R that serves as a knob to control the diode's polarity. Notably, the nonlocal diode's polarity can also be controlled by the strength of d_{xy}-wave altermagnetism, which can be seen by noting the change in the sign of η_L with J_1 in Fig. 7(b) [see also Fig. 7(c)]. This implies that d_{xy}-wave altermagnetism acts a switcher to turn on and off the nonlocal Josephson diode effect, in the same way as $d_{x^2-y^2}$-wave altermagnetism shown in Figs. 3(b) and 3(c). While there exist some similarities in how the diode's quality factor responds to both types of altermagnetic symmetries, the field strengths needed for manipulating the polarity are lower in coupled JJs with d_{xy}-wave altermagnetism, but larger efficiencies are supported with $d_{x^2-y^2}$-wave altermagnetism.

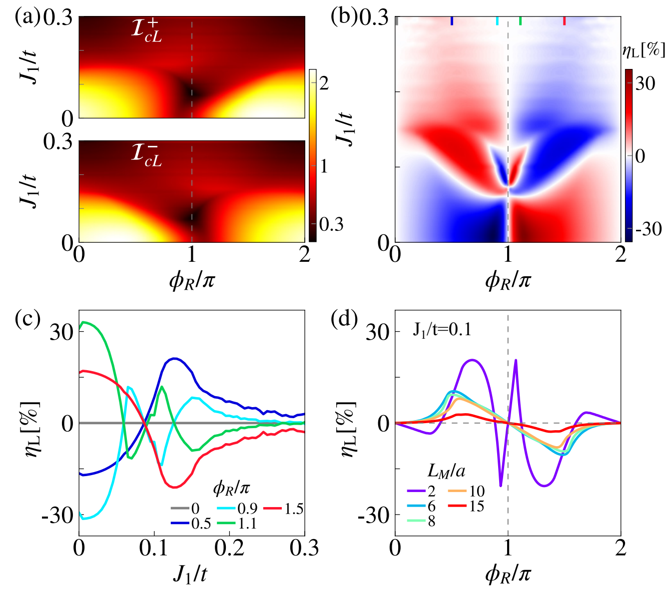

FIG. 7. (a) Critical currents $\mathcal{I}_{cL}^{\pm}$ as a function of ϕ_R and J_1 under d_{xy}-wave altermagnetism. (b) Quality factor η_L as a function of J_1 and ϕ_R. (c), (d) Line cuts of panels (b) for distinct values of J_1 and ϕ_R. The values of ϕ_R for the line cuts in panel (c) are marked by color bars in panel (b). Parameters: $L_M = 2a$ and the rest is the same as in Fig. 1.

[1] Y. Fukaya, B. Lu, K. Yada, Y. Tanaka, and J. Cayao, Superconducting phenomena in systems with unconventional magnets, J. Phys.: Condens. Matter **37**, 313003 (2025).

[2] Z. Liu, H. Hu, and X.-J. Liu, Altermagnetism and superconductivity: A short historical review, arXiv:2510.09170.

[3] Y. Noda, K. Ohno, and S. Nakamura, Momentum-dependent band spin splitting in semiconducting MnO_2: A density functional calculation, Phys. Chem. Chem. Phys. **18**, 13294 (2016).

[4] M. Naka, S. Hayami, H. Kusunose, Y. Yanagi, Y. Motome, and H. Seo, Spin current generation in organic antiferromagnets, Nat. Commun. **10**, 4305 (2019).

[5] S. Hayami, Y. Yanagi, and H. Kusunose, Momentum-dependent spin splitting by collinear antiferromagnetic ordering, J. Phys. Soc. Jpn. **88**, 123702 (2019).

[6] K.-H. Ahn, A. Hariki, K.-W. Lee, and J. Kuneš, Antiferromagnetism in RuO_2 as d-wave Pomeranchuk instability, Phys. Rev. B **99**, 184432 (2019).

[7] L.-D. Yuan, Z. Wang, J.-W. Luo, E. I. Rashba, and A. Zunger, Giant momentum-dependent spin splitting in centrosymmetric low-z antiferromagnets, Phys. Rev. B **102**, 014422 (2020).

[8] L. Šmejkal, R. González-Hernández, T. Jungwirth, and J. Sinova, Crystal time-reversal symmetry breaking and spontaneous Hall effect in collinear antiferromagnets, Sci. Adv. **6**, eaaz8809 (2020).

[9] M. Naka, S. Hayami, H. Kusunose, Y. Yanagi, Y. Motome, and H. Seo, Anomalous Hall effect in κ-type organic antiferromagnets, Phys. Rev. B **102**, 075112 (2020).

[10] L.-D. Yuan, Z. Wang, J.-W. Luo, and A. Zunger, Prediction of low-z collinear and noncollinear antiferromagnetic compounds having momentum-dependent spin splitting even without spin-orbit coupling, Phys. Rev. Mater. **5**, 014409 (2021).

[11] L. Šmejkal, J. Sinova, and T. Jungwirth, Beyond conventional ferromagnetism and antiferromagnetism: A phase with nonrelativistic spin and crystal rotation symmetry, Phys. Rev. X **12**, 031042 (2022).

[12] I. Mazin (The PRX Editors), Editorial: Altermagnetism—A new punch line of fundamental magnetism, Phys. Rev. X **12**, 040002 (2022).

[13] L. Šmejkal, J. Sinova, and T. Jungwirth, Emerging research landscape of altermagnetism, Phys. Rev. X **12**, 040501 (2022).

[14] H.-Y. Ma, M. Hu, N. Li, J. Liu, W. Yao, J.-F. Jia, and J. Liu, Multifunctional antiferromagnetic materials with giant piezomagnetism and noncollinear spin current, Nat. Commun. **12**, 2846 (2021).

[15] I. I. Mazin, Notes on altermagnetism and superconductivity, AAPPS Bull. **35**, 18 (2025).

[16] C. Song, H. Bai, Z. Zhou, L. Han, H. Reichlova, J. H. Dil, J. Liu, X. Chen, and F. Pan, Altermagnets as a new class of functional materials, Nat. Rev. Mater. **10**, 473 (2025).

[17] M. H. Devoret, A. Wallraff, and J. M. Martinis, Superconducting qubits: A short review, arXiv:cond-mat/0411174.

[18] J. Clarke and F. K. Wilhelm, Superconducting quantum bits, Nature (London) **453**, 1031 (2008).

[19] T. Brecht, W. Pfaff, C. Wang, Y. Chu, L. Frunzio, M. H. Devoret, and R. J. Schoelkopf, Multilayer microwave integrated quantum circuits for scalable quantum computing, npj Quantum Inf. **2**, 16002 (2016).

[20] P. Krantz, M. Kjaergaard, F. Yan, T. P. Orlando, S. Gustavsson, and W. D. Oliver, A quantum engineer's guide to superconducting qubits, Appl. Phys. Rev. **6**, 021318 (2019).

[21] J. M. Martinis, M. H. Devoret, and J. Clarke, Quantum Josephson junction circuits and the dawn of artificial atoms, Nat. Phys. **16**, 234 (2020).

[22] R. Aguado, A perspective on semiconductor-based superconducting qubits, Appl. Phys. Lett. **117**, 240501 (2020).

[23] M. Benito and G. Burkard, Hybrid superconductor-semiconductor systems for quantum technology, Appl. Phys. Lett. **116**, 190502 (2020).

[24] R. Aguado and L. P. Kouwenhoven, Majorana qubits for topological quantum computing, Phys. Today **73**(6), 44 (2020).

[25] J. Cayao, C. Triola, and A. M. Black-Schaffer, Odd-frequency superconducting pairing in one-dimensional systems, Eur. Phys. J. Spec. Top. **229**, 545 (2020).

[26] S. Rasmussen, K. Christensen, S. Pedersen, L. Kristensen, T. Bækkegaard, N. Loft, and N. Zinner, Superconducting circuit companion—An introduction with worked examples, PRX Quantum **2**, 040204 (2021).

[27] I. Siddiqi, Engineering high-coherence superconducting qubits, Nat. Rev. Mater. **6**, 875 (2021).

[28] A. Bargerbos, M. Pita-Vidal, R. Žitko, J. Ávila, L. J. Splitthoff, L. Grünhaupt, J. J. Wesdorp, C. K. Andersen, Y. Liu, L. P. Kouwenhoven, R. Aguado, A. Kou, and B. van Heck, Singlet-doublet transitions of a quantum dot Josephson junction detected in a transmon circuit, PRX Quantum **3**, 030311 (2022).

[29] M. Kjaergaard, M. E. Schwartz, J. Braumüller, P. Krantz, J. I.-J. Wang, S. Gustavsson, and W. D. Oliver, Superconducting qubits: Current state of play, Annu. Rev. Condens. Matter Phys. **11**, 369 (2020).

[30] M. Pita-Vidal, A. Bargerbos, R. Žitko, L. J. Splitthoff, L. Grünhaupt, J. J. Wesdorp, Y. Liu, L. P. Kouwenhoven, R. Aguado, B. van Heck, *et al.*, Direct manipulation of a superconducting spin qubit strongly coupled to a transmon qubit, Nat. Phys. **19**, 1110 (2023).

[31] Y. Tanaka, S. Tamura, and J. Cayao, Theory of Majorana zero modes in unconventional superconductors, Prog. Theor. Exp. Phys. **2024**, 08C105 (2024).

[32] J. A. Ouassou, A. Brataas, and J. Linder, Dc Josephson effect in altermagnets, Phys. Rev. Lett. **131**, 076003 (2023).

[33] C. W. J. Beenakker and T. Vakhtel, Phase-shifted Andreev levels in an altermagnet Josephson junction, Phys. Rev. B **108**, 075425 (2023).

[34] Y. Fukaya, K. Maeda, K. Yada, J. Cayao, Y. Tanaka, and B. Lu, Josephson effect and odd-frequency pairing in superconducting junctions with unconventional magnets, Phys. Rev. B **111**, 064502 (2025).

[35] S. Vosoughi-nia and M. P. Nowak, Altermon: A magnetic-field-free parity protected qubit based on a narrow altermagnet Josephson junction, arXiv:2510.18145.

[36] S.-B. Zhang, L.-H. Hu, and T. Neupert, Finite-momentum Cooper pairing in proximitized altermagnets, Nat. Commun. **15**, 1801 (2024).

[37] G. Z. Yang, Z.-T. Sun, Y.-M. Xie, and K. Law, Topological altermagnetic Josephson junctions, npj Quantum Mater. **11**, 45 (2026).

[38] B. Lu, K. Maeda, H. Ito, K. Yada, and Y. Tanaka, φ Josephson junction induced by altermagnetism, Phys. Rev. Lett. **133**, 226002 (2024).

[39] Q. Cheng and Q.-F. Sun, Orientation-dependent Josephson effect in spin-singlet superconductor/altermagnet/spin-triplet superconductor junctions, Phys. Rev. B **109**, 024517 (2024).

[40] H.-P. Sun, S.-B. Zhang, C.-A. Li, and B. Trauzettel, Tunable second harmonic in altermagnetic Josephson junctions, Phys. Rev. B **111**, 165406 (2025).

[41] W. Zhao, Y. Fukaya, P. Burset, J. Cayao, Y. Tanaka, and B. Lu, Orientation-dependent transport in junctions formed by d-wave altermagnets and d-wave superconductors, Phys. Rev. B **111**, 184515 (2025).

[42] M. Alipourzadeh and Y. Hajati, Andreev bound states and supercurrent in an unconventional superconductor-altermagnet Josephson junction, Phys. Rev. B **111**, 214515 (2025).

[43] A. Pal, D. Mondal, T. Nag, and A. Saha, Josephson current signature of Floquet Majorana and topological accidental zero modes in altermagnet heterostructures, Phys. Rev. B **112**, L201408 (2025).

[44] Q. Cheng, Y. Mao, and Q.-F. Sun, Field-free Josephson diode effect in altermagnet/normal metal/altermagnet junctions, Phys. Rev. B **110**, 014518 (2024).
[45] Y. Jiang, H.-L. Liu, and J. Wang, Josephson diode effect in altermagnet-based *s*-wave superconductor junction, Chin. Phys. B **34**, 107803 (2025).
[46] L. Sharma and M. Thakurathi, Tunable Josephson diode effect in singlet superconductor-altermagnet-triplet superconductor junctions, Phys. Rev. B **112**, 104506 (2025).
[47] D. Debnath, A. Saha, and P. Dutta, Spin polarization and diode effect in thermoelectric current through altermagnet-based superconductor heterostructures, Phys. Rev. B **113**, 104508 (2026).
[48] L. Sharma, B. Ghimire, and M. Thakurathi, *p*-wave magnet driven field-free Josephson diode effect, arXiv:2602.16677.
[49] V. D. Esin, D. Y. Kazmin, Y. S. Barash, A. V. Timonina, N. N. Kolesnikov, and E. V. Deviatov, Josephson diode and spin-valve effects on the surface of altermagnet CrSb, JETP Lett. **123**, 556 (2026).
[50] D. Shaffer and A. Levchenko, Theories of superconducting diode effects, arXiv:2510.25864.
[51] J.-D. Pillet, V. Benzoni, J. Griesmar, J.-L. Smirr, and Ç. Ö. Girit, Nonlocal Josephson effect in Andreev molecules, Nano Lett. **19**, 7138 (2019).
[52] J.-D. Pillet, V. Benzoni, J. Griesmar, J.-L. Smirr, and Ç. Ö. Girit, Scattering description of Andreev molecules, SciPost Phys. Core **2**, 009 (2020).
[53] H.-Y. Xie, M. G. Vavilov, and A. Levchenko, Weyl nodes in Andreev spectra of multiterminal Josephson junctions: Chern numbers, conductances, and supercurrents, Phys. Rev. B **97**, 035443 (2018).
[54] R. Mélin, Inversion in a four-terminal superconducting device on the quartet line. I. Two-dimensional metal and the quartet beam splitter, Phys. Rev. B **102**, 245435 (2020).
[55] R. Mélin, Ultralong-distance quantum correlations in three-terminal Josephson junctions, Phys. Rev. B **104**, 075402 (2021).
[56] E. W. Hodt and J. Linder, On-off switch and sign change for a nonlocal Josephson diode in spin-valve Andreev molecules, Phys. Rev. B **108**, 174502 (2023).
[57] J. Cayao, P. Burset, and Y. Tanaka, Controllable odd-frequency Cooper pairs in multisuperconductor Josephson junctions, Phys. Rev. B **109**, 205406 (2024).
[58] J.-D. Pillet, S. Annabi, A. Peugeot, H. Riechert, E. Arrighi, J. Griesmar, and L. Bretheau, Josephson diode effect in Andreev molecules, Phys. Rev. Res. **5**, 033199 (2023).
[59] F. Matute-Cañadas, L. Tosi, and A. L. Yeyati, Quantum circuits with multiterminal Josephson-Andreev junctions, PRX Quantum **5**, 020340 (2024).
[60] M. Kocsis, Z. Scherübl, G. H. Fülöp, P. Makk, and S. Csonka, Strong nonlocal tuning of the current-phase relation of a quantum dot based Andreev molecule, Phys. Rev. B **109**, 245133 (2024).
[61] J. Cayao and M. Sato, Non-Hermitian multiterminal phase-biased Josephson junctions, Phys. Rev. B **110**, 235426 (2024).
[62] J. H. Correa and M. P. Nowak, Theory of universal diode effect in three-terminal Josephson junctions, SciPost Phys. **17**, 037 (2024).
[63] P. Kotetes, M. Roig, and B. M. Andersen, Nonreciprocal equilibrium Josephson effect of arbitrary periodicity from poor man's Majorana zero modes, Phys. Rev. B **113**, L241403 (2026).
[64] G. A. Bobkov, D. S. Rabinovich, A. M. Bobkov, and I. V. Bobkova, Gate-tunable nonlocal Josephson effect through magnetic van der Waals bilayers, Phys. Rev. B **111**, 024506 (2025).
[65] J. Cayao and M. Sato, Nonlocal Josephson diode effect in minimal Kitaev chains, Phys. Rev. Res. **8**, 013326 (2026).
[66] E. Strambini, S. D'ambrosio, F. Vischi, F. Bergeret, Y. V. Nazarov, and F. Giazotto, The ω-squipt as a tool to phase-engineer Josephson topological materials, Nat. Nanotechnol. **11**, 1055 (2016).
[67] Z. Su, A. B. Tacla, M. Hocevar, D. Car, S. R. Plissard, E. P. A. M. Bakkers, A. J. Daley, D. Pekker, and S. M. Frolov, Andreev molecules in semiconductor nanowire double quantum dots, Nat. Commun. **8**, 585 (2017).
[68] A. W. Draelos, M.-T. Wei, A. Seredinski, H. Li, Y. Mehta, K. Watanabe, T. Taniguchi, I. V. Borzenets, F. Amet, and G. Finkelstein, Supercurrent flow in multiterminal graphene Josephson junctions, Nano Lett. **19**, 1039 (2019).
[69] N. Pankratova, H. Lee, R. Kuzmin, K. Wickramasinghe, W. Mayer, J. Yuan, M. G. Vavilov, J. Shabani, and V. E. Manucharyan, Multiterminal Josephson effect, Phys. Rev. X **10**, 031051 (2020).
[70] G. V. Graziano, M. Gupta, M. Pendharkar, J. T. Dong, C. P. Dempsey, C. Palmstrøm, and V. S. Pribiag, Selective control of conductance modes in multi-terminal Josephson junctions, Nat. Commun. **13**, 5933 (2022).
[71] S. Matsuo, J. S. Lee, C.-Y. Chang, Y. Sato, K. Ueda, C. J. Palmstrøm, and S. Tarucha, Observation of nonlocal Josephson effect on double InAs nanowires, Commun. Phys. **5**, 221 (2022).
[72] C. Jünger, S. Lehmann, K. A. Dick, C. Thelander, C. Schönenberger, and A. Baumgartner, Intermediate states in Andreev bound state fusion, Commun. Phys. **6**, 190 (2023).
[73] S. Matsuo, T. Imoto, T. Yokoyama, Y. Sato, T. Lindemann, S. Gronin, G. C. Gardner, M. J. Manfra, and S. Tarucha, Phase engineering of anomalous Josephson effect derived from Andreev molecules, Sci. Adv. **9**, eadj3698 (2023).
[74] S. Matsuo, T. Imoto, T. Yokoyama, Y. Sato, T. Lindemann, S. Gronin, G. C. Gardner, S. Nakosai, Y. Tanaka, M. J. Manfra, *et al.*, Phase-dependent Andreev molecules and superconducting gap closing in coherently-coupled Josephson junctions, Nat. Commun. **14**, 8271 (2023).
[75] D. Z. Haxell, M. Coraiola, M. Hinderling, S. C. ten Kate, D. Sabonis, A. E. Svetogorov, W. Belzig, E. Cheah, F. Krizek, R. Schott, W. Wegscheider, and F. Nichele, Demonstration of the nonlocal Josephson effect in Andreev molecules, Nano Lett. **23**, 7532 (2023).
[76] D. van Driel, B. Roovers, F. Zatelli, A. Bordin, G. Wang, N. van Loo, J. C. Wolff, G. P. Mazur, S. Gazibegovic, G. Badawy, E. P. Bakkers, L. P. Kouwenhoven, and T. Dvir, Charge sensing the parity of an Andreev molecule, PRX Quantum **5**, 020301 (2024).
[77] S. Zhu, Y. Ma, J. He, X. Yang, Z. Jia, M. Wei, Y. Jiao, J. He, E. Zhuo, X. Cao, *et al.*, Josephson diode effect in nanowire-based Andreev molecules, Commun. Phys. **8**, 330 (2025).
[78] R.-P. Riwar, M. Houzet, J. S. Meyer, and Y. V. Nazarov, Multi-terminal Josephson junctions as topological matter, Nat. Commun. **7**, 11167 (2016).

[79] F. Pientka, A. Keselman, E. Berg, A. Yacoby, A. Stern, and B. I. Halperin, Topological superconductivity in a planar Josephson junction, Phys. Rev. X **7**, 021032 (2017).
[80] J. Hu, C. Wu, and X. Dai, Proposed design of a Josephson diode, Phys. Rev. Lett. **99**, 067004 (2007).
[81] F. Dolcini, M. Houzet, and J. S. Meyer, Topological Josephson ϕ_0 junctions, Phys. Rev. B **92**, 035428 (2015).
[82] K. N. Nesterov, M. Houzet, and J. S. Meyer, Anomalous Josephson effect in semiconducting nanowires as a signature of the topologically nontrivial phase, Phys. Rev. B **93**, 174502 (2016).
[83] K. Misaki and N. Nagaosa, Theory of the nonreciprocal Josephson effect, Phys. Rev. B **103**, 245302 (2021).
[84] Y. Tanaka, B. Lu, and N. Nagaosa, Theory of giant diode effect in d-wave superconductor junctions on the surface of a topological insulator, Phys. Rev. B **106**, 214524 (2022).
[85] M. Davydova, S. Prembabu, and L. Fu, Universal Josephson diode effect, Sci. Adv. **8**, eabo0309 (2022).
[86] S. Mondal, P.-H. Fu, and J. Cayao, Josephson diode effect with Andreev and Majorana bound states, Phys. Rev. B **112**, 144506 (2025).
[87] J. Cayao, N. Nagaosa, and Y. Tanaka, Enhancing the Josephson diode effect with Majorana bound states, Phys. Rev. B **109**, L081405 (2024).
[88] R. Seoane Souto, M. Leijnse, C. Schrade, M. Valentini, G. Katsaros, and J. Danon, Tuning the Josephson diode response with an ac current, Phys. Rev. Res. **6**, L022002 (2024).
[89] Z. Liu, L. Huang, and J. Wang, Josephson diode effect in topological superconductors, Phys. Rev. B **110**, 014519 (2024).
[90] Y. Zhang, Y. Gu, P. Li, J. Hu, and K. Jiang, General theory of Josephson diodes, Phys. Rev. X **12**, 041013 (2022).
[91] C. Beenakker, Three "universal" mesoscopic Josephson effects, in *Transport Phenomena in Mesoscopic Systems: Proceedings of the 14th Taniguchi Symposium, Shima, Japan, November 10–14, 1991* (Springer, Berlin, 1992), Vol. 109, p. 235.
[92] A. Zagoskin, *Quantum Theory of Many-Body Systems: Techniques and Applications* (Springer, Berlin, 2014).
[93] A. Furusaki and M. Tsukada, Dc Josephson effect and Andreev reflection, Solid State Commun. **78**, 299 (1991).
[94] A. Furusaki, Josephson current carried by Andreev levels in superconducting quantum point contacts, Superlattices Microstruct. **25**, 809 (1999).
[95] S. Kashiwaya and Y. Tanaka, Tunnelling effects on surface bound states in unconventional superconductors, Rep. Prog. Phys. **63**, 1641 (2000).
[96] J. Cayao, P. San-Jose, A. M. Black-Schaffer, R. Aguado, and E. Prada, Majorana splitting from critical currents in Josephson junctions, Phys. Rev. B **96**, 205425 (2017).
[97] J. Cayao, A. M. Black-Schaffer, E. Prada, and R. Aguado, Andreev spectrum and supercurrents in nanowire-based SNS junctions containing Majorana bound states, Beilstein J. Nanotechnol. **9**, 1339 (2018).
[98] O. A. Awoga, J. Cayao, and A. M. Black-Schaffer, Supercurrent detection of topologically trivial zero-energy states in nanowire junctions, Phys. Rev. Lett. **123**, 117001 (2019).
[99] J. Cayao and A. M. Black-Schaffer, Distinguishing trivial and topological zero-energy states in long nanowire junctions, Phys. Rev. B **104**, L020501 (2021).
[100] A. A. Golubov, M. Y. Kupriyanov, and E. Il'ichev, The current-phase relation in Josephson junctions, Rev. Mod. Phys. **76**, 411 (2004).
[101] K. Maeda, Y. Fukaya, K. Yada, B. Lu, Y. Tanaka, and J. Cayao, Classification of pair symmetries in superconductors with unconventional magnetism, Phys. Rev. B **111**, 144508 (2025).
[102] D. Chakraborty and A. M. Black-Schaffer, Constraints on superconducting pairing in altermagnets, Phys. Rev. B **112**, 014516 (2025).
[103] M. Khodas, S. Mu, I. I. Mazin, and K. D. Belashchenko, Tuning of altermagnetism by strain, Phys. Rev. B **113**, 104422 (2026).
[104] X. Feng and Z. Zhang, Superconducting order parameters in spin space groups: Methodology and application, Phys. Rev. B **111**, 054520 (2025).
[105] K. Parshukov and A. P. Schnyder, Exotic superconducting states in altermagnets, arXiv:2507.10700.
[106] P.-H. Fu, S. Mondal, J.-F. Liu, and J. Cayao, Light-induced Floquet spin-triplet Cooper pairs in unconventional magnets, SciPost Phys. **20**, 059 (2026).
[107] P.-H. Fu, S. Mondal, J.-F. Liu, Y. Tanaka, and J. Cayao, Floquet engineering spin triplet states in unconventional magnets, Phys. Rev. Lett. **136**, 066703 (2026).
[108] T. Yokoyama, Floquet engineering triplet superconductivity in superconductors with spin-orbit coupling or altermagnetism, Phys. Rev. B **112**, 024512 (2025).
[109] K. Mukasa and Y. Masaki, Finite-momentum superconductivity in two-dimensional altermagnets with a Rashba-type spin–orbit coupling, J. Phys. Soc. Jpn. **94**, 064705 (2025).
[110] N. Heinsdorf and M. Franz, Proximitizing altermagnets with conventional superconductors, Phys. Rev. B **113**, L020501 (2026).
[111] K. Monkman, J. Weng, N. Heinsdorf, A. Nocera, Y. Barlas, and M. Franz, Persistent spin currents in superconducting altermagnets, Phys. Rev. X **16**, 011057 (2026).
[112] J. Chang, H. Lu, J. Zhao, H.-G. Luo, and Y. Ding, Energy dispersion, superconductivity, and magnetic fluctuations in stacked altermagnetic materials, Phys. Rev. B **111**, 104432 (2025).
[113] M. Khodas, L. Šmejkal, and I. I. Mazin, Nonrelativistic-Ising superconductivity in p-wave magnets, Phys. Rev. B **114**, L080505 (2026).
[114] B. Lu, P. Mercebach, P. Burset, K. Yada, J. Cayao, Y. Tanaka, and Y. Fukaya, Engineering subgap states in superconductors by altermagnetism, Phys. Rev. B **113**, L180501 (2026).
[115] Z. Liu, H. Hu, and X. -J. Liu, Fulde-Ferrell-Larkin-Ovchinnikov states and topological Bogoliubov Fermi surfaces in altermagnets: An analytical study, Phys. Rev. B **113**, 024518 (2026).
[116] Y. Fukaya, B. Lu, K. Yada, Y. Tanaka, and J. Cayao, Crossed surface flat bands in three-dimensional superconducting altermagnets, Phys. Rev. Lett. **136**, 226001 (2026).